Inversion of Spin Polarization and Tunneling Magnetoresistance in Spin-Dependent Tunneling Junctions

Manish Sharma,[1] Shan X. Wang,[1,2,*] and Janice H. Nickel[3]
[1]Electrical Engineering, Stanford University, Stanford, California 94305-2205
[2]Materials Science & Engineering, Stanford University, Stanford, California 94305-2205
[3]Hewlett-Packard Laboratories, 1501 Page Mill Road 5L-D, Palo Alto, California 94304-1126
(Received 6 May 1998)

An inversion of spin polarization has been observed in spin-dependent tunneling (SDT) junctions with Ta_2O_5 and Ta_2O_5/Al_2O_3 barriers. The resistance of an SDT junction is found to be lower with magnetization of the ferromagnetic electrodes aligned antiparallel under specific voltage configurations. The tunneling magnetoresistance effect changes sign with applied voltage and varies from +1% to −4% at room temperature. This inversion is believed to be due to the change in sign with bias of the spin polarization of one of the two electrodes. The strong dependence on voltage suggests negative spin polarization could arise from the densities of states for spins being different at the two electrode/barrier interfaces. [S0031-9007(98)08200-3]

PACS numbers: 73.40.Gk, 75.70.Pa, 85.30.Mn

Spin-dependent tunneling (SDT) between ferromagnetic (FM) electrodes across an insulating barrier was first reported by Julliere [1]. He observed a 14% change in the resistance of an SDT junction of Fe and Co electrodes separated by a Ge barrier. A model of the spin polarization of the tunneling electrons proposed earlier by Tedrow and Meservey [2,3] was used to suggest a simple formula for the tunneling magnetoresistance (TMR) ratio:

$$\Delta R/R_p = R_{ap}/R_p - 1 = 2P_1P_2/(1 - P_1P_2),$$

where R_{ap} is the resistance of the SDT junction with the magnetizations of the ferromagnetic electrodes aligned antiparallel to each other, and R_p is the resistance with magnetizations aligned parallel. Here, $P_\sigma = (k_{\sigma\uparrow} - k_{\sigma\downarrow})/(k_{\sigma\uparrow} + k_{\sigma\downarrow})$ is the spin polarization coefficient of electrode $\sigma = 1, 2$ with $k_{\sigma\uparrow}$ and $k_{\sigma\downarrow}$ being the free-electron wave vectors of the tunneling electrons close to the Fermi level [2–4]. The SDT effect has recently attracted much interest due to success in both achieving high TMR ratios and forming tunneling barriers with good reproducibility [5–16]. Critical to the SDT material system is the choice of the tunneling barrier. Only a few materials form good barriers for spin-polarized tunneling: Al_2O_3 [5–13], AlN [9], GdO_x [14,15], NiO [14], MgO [16], and HfO_2 [16]. Amongst these, Al_2O_3 has proved to be the most successful in SDT junctions [5–7]. This is largely attributed to the excellent wetting properties of Al and its ability to oxidize readily. Reactively sputtered Ta_2O_5 has been attempted in SDT junctions by Platt *et al.* [16], albeit without success.

We have successfully fabricated Ta_2O_5 and composite Ta_2O_5/Al_2O_3 SDT junctions. In this Letter, we report on SDT junctions using plasma-oxidized Ta/Al to form a composite Ta_2O_5/Al_2O_3 barrier. The TMR ratios of these junctions are found to be strongly dependent on the applied voltage. A negative TMR effect is observed over a wide range of negative voltages for junctions with Ta_2O_5/Al_2O_3 barriers. A positive TMR effect is observed in these junctions when the applied voltage is greater than −0.1 V. For junctions with barriers of reversed composition, i.e., Al_2O_3/Ta_2O_5, this TMR behavior is reversed. These results indicate that the spin polarization coefficient at the Ta_2O_5/electrode interface is of opposite sign than that at the Al_2O_3/electrode interface under specific bias conditions.

A Sputtered Films Shamrock deposition system was used to deposit the SDT structures on Si substrates. The bottom electrode was 12-nm-thick $Ni_{80}Fe_{20}$ exchange biased with an underlying 10-nm-thick FeMn layer. Thin layers of Ta and/or Al were deposited above the bottom electrode in thicknesses varying from 0.5 to 1.5 nm and plasma oxidized *in situ* to form the barrier. Processing conditions for the samples are given in Table I. An 8 nm NiFe layer was used as the counterelectrode. Photolithography was used to pattern the junctions in sizes of 5 μm × 10 μm, 10 μm × 20 μm, and 30 μm × 60 μm. Magnetoresistance measurements were done using a Keithley S110 Hall Effect System in conjunction with a CTI-Cryogenics C22 Helium compressor. In addition, x-ray photoelectron spectroscopy was used to study detailed oxidation states of the barrier by depth profiling. Results of these experiments and more detailed studies of oxidation times and barrier thicknesses are being published elsewhere [17,18].

Figure 1 shows the resistance of a 5 μm × 10 μm junction from sample set *A* as a function of the applied magnetic field under various applied voltages. The barrier in sample set *A* was formed by depositing layers of Ta (0.5 nm) and Al (0.5 nm) and then oxidizing for 1 min. The voltage applied corresponds to positive bias with respect to the top electrode (in this case, the Al_2O_3 side of the barrier). The usual magnetic exchange-biased loop is seen with an exchange bias of ~150 Oe. The free layer loop is slightly offset from zero field due to ferromagnetic

 0031-9007/99/82(3)/616(4)$15.00 © 1999 The American Physical Society

TABLE I. TMR ($\Delta R/R$) and R results for samples with different barriers. Values are for 5 μm × 10 μm sized junctions. Data for both room (297 K) and low (20–30 K) temperature measurements are shown. Maximum positive and inverse $\Delta R/R$ values observed are shown separately.

Sample	*A*	*B*	*C*	*D*	*E*
Barrier layer (nm)	Ta 0.5/Al 0.5	Ta 0.75/Al 0.75	Al 0.75/Ta 0.75	Ta 0.75	Al 1.25
Oxidation time (min)	1	4	4	1.5	2.5
At room temp:					
R (MΩ μm^2)	0.05	107	61	1.28	0.13
Max $\Delta R/R$(%)	1.8	1.2	2.0	1.0	16
	−2.2	−4.1	−0.8	−0.7	···
At low temp:					
R (MΩ μm^2)	0.06	140	135	···	···
Max $\Delta R/R$(%)	2.7	2.2	4.0	···	···
	−3.2	−7.2	−1.0	···	···

coupling with the exchange-biased layer. The magnetic moments of the electrodes are aligned antiparallel to each other for fields between 15–150 Oe and are parallel for higher and lower fields. At −0.43 V, the junctions have a lower resistance for antiparallel alignment, demonstrating an inverse TMR effect. As the applied voltage is raised, the magnitude of inverse TMR is reduced, the junctions exhibiting zero magnetoresistance close to −0.11 V. Raising the voltage further induces a positive MR effect, which reaches a peak at +0.2 V and decreases at higher voltages.

The inverse TMR effect observed is rather striking. First, both the electrodes used are NiFe, with a well known positive spin polarization when measured through Al_2O_3 tunneling barriers. Second, the inversion occurs at small voltages (±0.5 V). The only previous predictions of negative spin polarization known to the authors are those reported for spin-polarized scanning tunneling microscopes with different tunneling tip and sample materials [19,20]. These are expected to occur at relatively higher voltages (>1 V). Third, this inversion is not likely to be an artifact of junction geometry as the junctions have high resistances (cf. Table I) and data were obtained by two-probe measurements. This is particularly evident as the contribution of the leads to the junction resistance is less than 150 Ω.

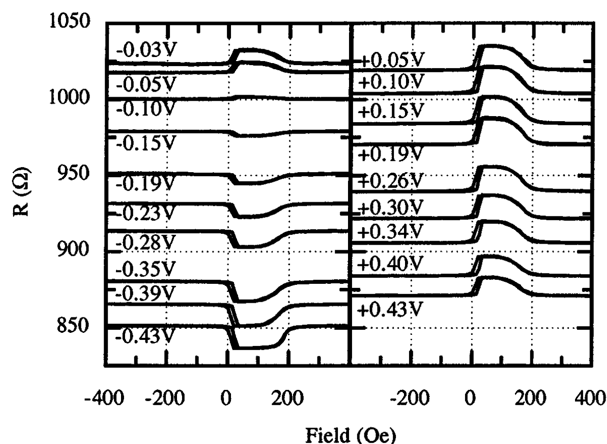

FIG. 1. Typical R-H plots obtained at 297 K for sample A (Ta 0.5 nm/Al 0.5 nm). An inverse TMR effect is seen below −0.11 V. Note the ordinate scale is in terms of absolute resistance. Because of the nonlinear I-V characteristic, resistance changes with applied bias and the curves shift vertically. Curves for positive bias are shown separately to the right for clarity.

Measurements of the bias dependence of TMR were performed over the entire possible voltage range. The breakdown voltage of most devices was greater than 1.5 V. Results of magnetotransport measurements are summarized in Table I. In Fig. 2 are shown TMR ratio versus applied bias curves typical for sample sets A, B, C, D, and E. Sample sets A and B [cf. Fig. 2(a)] exhibit negative TMR values for large negative voltages, i.e., when the Ta_2O_5 side of the barrier is positively biased. The I-V curves observed are slightly asymmetric indicating different barrier heights for the Ta_2O_5 and the Al_2O_3 sides of the barrier. For sample set C [cf. Fig. 2(b)], the negative excursion of TMR occurs at positive voltages. This is because, the Ta layer being deposited atop the Al layer, Ta_2O_5 now lies adjacent to the top electrode and is positively biased. It is possible that the magnitude of TMR differs from that in sample set B because the oxidation now occurs with the Ta layer atop the Al layer. In sample set D, a Ta-only barrier produces a negative-going excursion of TMR for high enough positive and negative voltages [cf. Fig. 2(c)]. This suggests that the TMR, being proportional to P_1P_2 near zero bias (as discussed in the following paragraphs), is positive for small voltages and changes sign at higher voltages. Sample set E with an Al-only barrier served as a control for our experiments. It exhibits the usual voltage dependence of TMR with a maximum TMR of 16% at room temperature [cf. Fig. 2(d)]. It is thus clear that the observed effects arise from changing the barrier material alone. A zero-bias anomaly, possibly related to different oxidation mechanisms, is also observed in some samples [18].

By matching free-electron wave functions at the electrode/barrier interface, Slonczewski extended the original

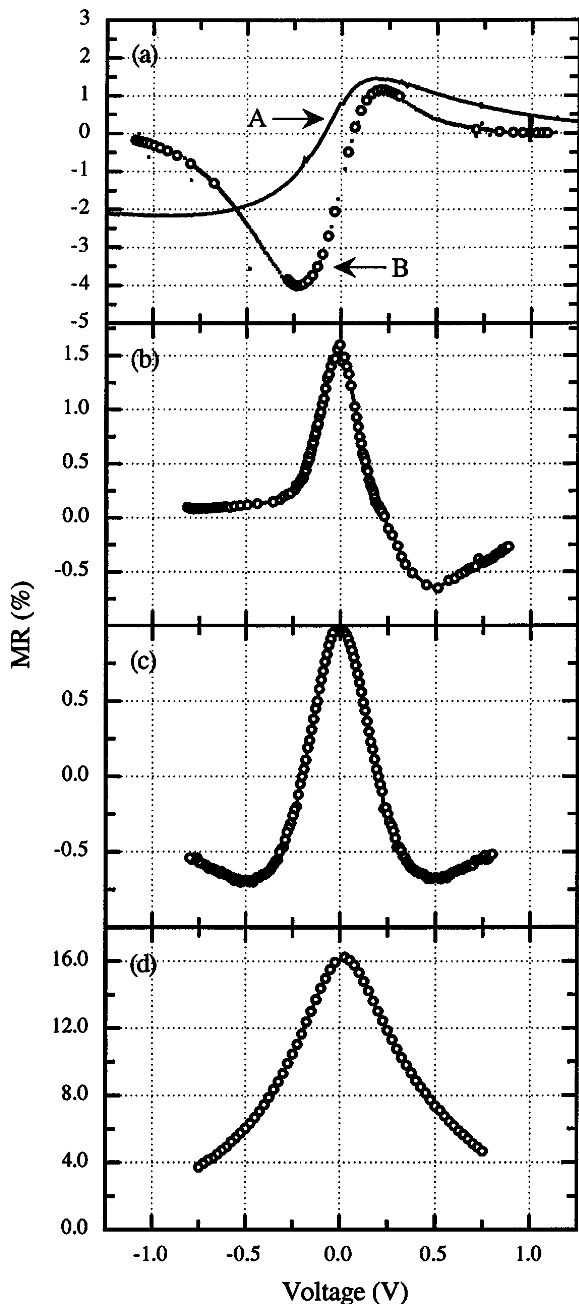

FIG. 2. Voltage dependence of TMR for (a) samples *A* (Ta 0.5 nm/Al 0.5 nm) and *B* (Ta 0.75 nm/Al 0.75 nm), (b) sample *C* (Al 0.75 nm/Ta 0.75 nm), (c) sample *D* (Ta 0.75 nm), and (d) sample *E* (Al 1.25 nm). Sample *A* exhibits negative TMR at negative bias and positive TMR for bias greater than −0.1 V. In sample *C*, the barrier composition is opposite that in samples *A* and *B* and the negative excursion of TMR occurs above +0.1 V. For sample *D*, a Ta-only barrier causes a negative excursion for both high enough positive and negative voltages. With an Al-only barrier, sample *E* served as a control and has the usual always positive TMR decaying at higher voltages.

definition of the spin polarization coefficient P_σ to propose possible contributions from electrode-barrier interface effects [21]:

$$P_\sigma = \frac{(k_{\sigma\uparrow} - k_{\sigma\downarrow})(\kappa^2 - k_{\sigma\uparrow}k_{\sigma\downarrow})}{(k_{\sigma\uparrow} + k_{\sigma\downarrow})(\kappa^2 + k_{\sigma\uparrow}k_{\sigma\downarrow})},$$

where κ, the wave vector in the barrier region, is taken to be the same for tunneling electrons of either spin. As discussed by Meservey and Tedrow, the observed TMR ratio, being proportional to P_1P_2, can be negative if the electrode spin polarizations, P_1 and P_2, given by the above equation are of opposite sign [6]. This could happen due to either of the two terms in the numerator. The above formulation has been modified by Bratkovsky to include contributions from effective mass [12].

Recently, in doing calculations of the spin-polarized surface densities of states for Co from first principles, Tsymbal and Pettifor have found the polarization of *s* electrons alone is of opposite sign from the combined polarization of *s*, *p*, and *d* electrons [22]. They conclude that the nature of the bonding at the electrode/insulator interface can influence the character of the tunneling electrons and thus both size and sign of the polarization.

In our studies, since the same material, NiFe, is used for both the top and bottom electrodes, it is possible that the interfaces have a profound effect on the tunneling of electrons. Because of the very different band structures of Ta_2O_5 and Al_2O_3, and consequently different bonding characteristics, the relative contribution from *s* electrons and from *d* electrons to the tunneling current could be markedly different at the two interfaces even though the electrode materials are the same. The character of tunneling electrons could change, thus giving the ferromagnetic electrodes spin polarizations of opposite signs.

The strong dependence of TMR at low voltages in our junctions suggests that an inversion similar to that predicted by Bürgler and Tarrach [20] could occur quite close to the Fermi level. A similar peaked feature 0.1–0.2 eV in width could produce the TMR curves of Fig. 2. We have done calculations along similar lines and incorporated the treatment of spins by Slonczewski [21] on a hypothetical band structure shown in Fig. 3(a). The shaded regions represent states lying between the two Fermi levels that contribute to the tunneling current. As can be seen, the spin polarizations of FM1 and FM2 are opposite in sign for a bias of −0.2 V, resulting in a negative TMR. In Fig. 3(b), when the bias is +0.2 V, both FM1 and FM2 have spin polarizations of the same sign, and the resultant TMR is positive. The full TMR versus bias curve is shown in Fig. 3(c). The general shape of this curve resembles closely the experimental curves obtained [cf. Fig. 2(a)]. To simplify the calculation, the effects of the effective mass of the tunneling electrons and the barrier shape due to differing barrier heights on the Ta and the Al sides were not included.

In summary, both Ta_2O_5 and composite Ta_2O_5/Al_2O_3 barrier junctions exhibit TMR effects of about 2% at room temperature and 4% at low temperatures. An inversion of magnetoresistance that is voltage dependent is observed in some Ta_2O_5 and composite Al_2O_3/Ta_2O_5 junctions.

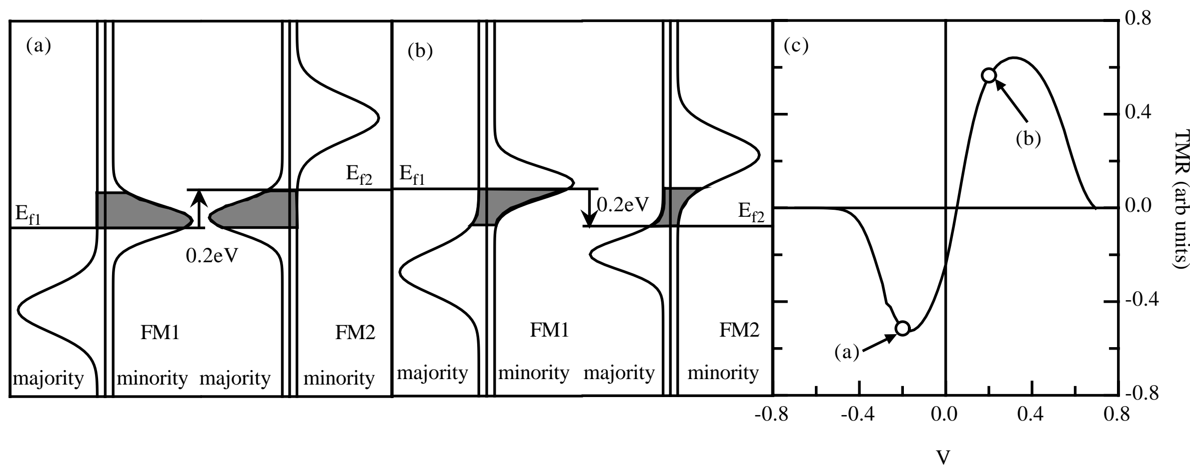

FIG. 3. Simple calculation for explaining inverse magnetoresistance. A hypothetical density of states mimicking gross features in calculated band structures is used here purely for illustration. The two metals, FM1 and FM2, have an exchange splitting of 0.5 eV and different band structures with E_{f1} higher than E_{f2} by about 0.3 eV. Shaded regions show portions of densities of states that take part in the tunneling process. (a) FM2 biased at -0.2 V with respect to FM1, (b) FM2 biased at $+0.2$ V, and (c) the resultant TMR versus bias curve. Note the general shape of the curve reproduces the features seen in the experimental data [cf. Fig. 2(a)].

The characteristics of the TMR versus voltage curve is reversed with respect to bias voltage for Al_2O_3/Ta_2O_5 barriers. These results suggest the polarization of the Ta_2O_5/electrode interface is of sign opposite to that of the Al_2O_3/electrode interface and changes with the applied bias. The magnitude of the inverse TMR effect is found to be influenced by the oxidation time of the samples. The nature of the bonding between the oxide and the electrode greatly influences the spin-polarized contributions from s- and d-band states. These results indicate that spin-polarized spectroscopic measurements of the densities of states near the Fermi level may be possible to determine the nature of the tunneling electrons.

The authors thank Tom Anthony and Mary West at HP Labs for help with the depositions of the SDT junctions and Evgueni Tsymbal, Shufeng Zhang, and Alex Bratkovsky for useful discussions of the results. M. S. also thanks Kyusik Sin for help in setting up the low-temperature measurements. This work is supported in part by the NSF-MRSEC program through the Center for Materials Research at Stanford University.

*Email: sxwang@ee.stanford.edu

[1] M. Julliere, Phys. Lett. **54A**, 225 (1975).
[2] P. M. Tedrow and R. Meservey, Phys. Rev. Lett. **26**, 192 (1971).
[3] R. Meservey, D. Paraskevopoulos, and P. M. Tedrow, Phys. Rev. Lett. **37**, 858 (1976).
[4] M. B. Stearns, J. Magn. Magn. Mater. **5**, 167 (1977).
[5] J. S. Moodera, L. R. Kinder, T. M. Wong, and R. Meservey, Phys. Rev. Lett. **74**, 3273 (1995).
[6] R. Meservey and P. M. Tedrow, Phys. Rep. **238**, 173 (1994).
[7] J. S. Moodera and L. R. Kinder, J. Appl. Phys. **79**, 4724 (1996).
[8] T. Miyazaki and N. Tezuka, J. Magn. Magn. Mater. **139**, L231 (1995).
[9] T. S. Plaskett, P. P. Freitas, J. J. Sun, R. C. Sousa, F. F. da Silva, T. T. P. Galvao, N. M. Pinho, S. Cardoso, M. F. da Silva, and J. C. Soares, in *Magnetic Ultrathin Films, Multilayers and Surfaces, San Francisco, 1997,* edited by J. Tobin, D. Chambliss, D. Kubinski, K. Barmak, P. Dederichs, W. de Jonge, T. Katayama, and A. Schuhl, MRS Symposia Proceedings No. 475 (Materials Research Society, Pittsburgh, 1997), pp. 469–474.
[10] T. Miyazaki, T. Yaoi, and S. Ishio, J. Magn. Magn. Mater. **98**, L7 (1991).
[11] W. J. Gallagher, S. S. P. Parkin, Yu Lu, X. P. Bian, A. Marley, R. A. Altman, S. A. Rishton, K. P. Roche, C. Jahnes, and T. M. Shaw, J. Appl. Phys. **81**, 3741 (1997).
[12] A. Bratkovsky, Phys. Rev. B **56**, 2344 (1997).
[13] A. Bratkovsky and J. H. Nickel, J. Magn. Soc. Jpn. (to be published).
[14] J. Nowak and J. Rauluszkiewicz, J. Magn. Magn. Mater. **109**, 79 (1992).
[15] M. Ohba, Y. Obi, K. Takanashi, and H. Fujimori, Sci. Rep. Res. Inst., Tohoku Univ., Ser. A **42**, 161 (1996).
[16] C. L. Platt, B. Dieny, and A. E. Berkowitz, J. Appl. Phys. **81**, 5523 (1997).
[17] M. Sharma, S. X. Wang, and J. H. Nickel, J. Appl. Phys. (to be published).
[18] M. Sharma, S. X. Wang, and J. H. Nickel (to be published).
[19] R. Wiesendanger, D. Bürgler, G. Tarrach, A. Wadas, D. Brodbeck, and H. J. Güntherodt, J. Vac. Sci. Technol. B **9**, 519 (1991).
[20] D. Bürgler and G. Tarrach, Ultramicroscopy **42–44**, 194 (1992).
[21] J. C. Slonczewski, Phys. Rev. B **39**, 6995 (1989).
[22] E. Yu Tsymbal and D. G. Pettifor, J. Phys. Condens. Matter **9**, L411 (1997).